

MORPHOMETRIC AND HEMODYNAMIC IMPACT OF POST ENDOVASCULAR AAA REPAIR: COMPARISON WITH INFRARENAL PHYSIOLOGICAL BLOOD FLOW

P. Tasso (1), A. Raptis (2), M. Xenos (2, 3), D. Gallo (1),
M. Matsagkas (2, 4), U. Morbiducci (1)

(1) Dept. of Mechanical and
Aerospace Engineering
Politecnico di Torino
Torino, Italy

(3) Dept. of Mathematics
University of Ioannina
Ioannina, Greece

(2) Institute of Vascular Diseases
Laboratory for Vascular Simulations
Ioannina, Greece

(4) Dept. of Vascular Surgery,
Faculty of Medicine,
University of Thessaly,
Larissa, Greece

INTRODUCTION

Abdominal aortic aneurysm (AAA) is a localized expansion of the abdominal aorta. Among treatments for AAA, endovascular aneurysm repair (EVAR) is a reliable technique which is a minimally invasive alternative to classical open-chest surgery. Technically, EVAR is performed by the endovascular delivery and deployment of an endovascular stent graft, to reinforce the wall of the abdominal aorta and to keep the damaged area from rupturing. EVAR of AAAs results in (1) redirection of blood through the deployed endograft, and in (2) reshape of the iliac bifurcation, altering local hemodynamics and adversely affecting its performance [1]. In the last decade post-EVAR effects have been investigated harnessing the power of computational methods [2]. However, the interplay between geometry and hemodynamics in AAAs pre- and post-treatment has been poorly investigated. Here we present a study on the impact of AAA endovascular repair on geometric features and local hemodynamics. The purpose is to define both geometric and hemodynamic features that deviate markedly from their physiological values after EVAR. In detail, local vascular geometric features like curvature, torsion, and cross-sectional area are evaluated in the pre- and post-operative geometries (1 month follow-up after stent graft implantation), and in healthy models. Near-wall flow quantities are calculated with CFD (Computational Fluid Dynamics), and related to the geometric features, to explore if the post interventional reshaping of the vascular territory supports the re-establishment of physiological hemodynamics.

METHODS

Ten subjects suffering from AAA underwent implantation of an Endurant® (Medtronic, Santa Rosa, CA, USA) stent-graft system at the University Hospital of Ioannina, Greece. Computed tomography

(CT) scans of the subjects were obtained before and one month after EVAR (as detailed in [1]). Five subjects with no sign of aneurysmal disease underwent CT angiography of the region including the abdominal aorta and common iliac arteries. DICOM images of all subjects were then segmented using Mimics (Materialise, Leuven, Belgium). The postoperative models were restricted to the deployed endovascular graft interior space (no extension to the suprarenal abdominal aorta or the native iliac arteries), while the preoperative and healthy models included the lumen between the renal arteries and the iliac bifurcation [2]. On the reconstructed 3D models, a morphometric analysis based on the geometric centerline was carried out. Centerlines were extracted as the geometrical locus of the centers of the maximum inscribed spheres in the model, as given by the Vascular Modelling Toolkit software (VMTK). Free-knots regression splines were then employed as a basis of representation to provide a noise free, analytical formulation of the centerlines [2]. By differentiation of the free-knots regression spline representations, centerlines were characterized in terms of curvature and torsion, that are known to have a major influence on hemodynamics. Cross-sectional area $A(s)$ along the curvilinear abscissa s were calculated automatically via intersection of a plane normal to the centerline. The reconstructed 3D geometries were meshed with tetrahedral elements [1]. The unsteady incompressible blood flow equations were solved by using the finite volume-based method software package Ansys Fluent (Ansys Inc., Canonsburg, PA). Blood was considered as Newtonian, incompressible fluid. Boundary conditions at inflow and outflow sections were based on flow and pressure measurements by Olufsen et al. [3]. More in detail, a physiological pulse pressure condition was applied as Neumann inflow boundary condition in all the models, while an outflow section area-based flow split strategy was applied at the outflow sections. Near-wall hemodynamics was described in terms

of wall shear stress, while intravascular flow structures were described in terms of helical flow.

RESULTS

Local curvature profiles calculated along healthy and post-operative models provide a clear representation of the impact that the stenting procedure had in reshaping the vessel, the final goal being reestablishing healthy geometric features (Fig. 1). The group averaged values of curvature and cross-sectional area diminished from pre- to post-operative geometries. However, post-operative geometric features still differ from healthy models (Fig. 2a-2b).

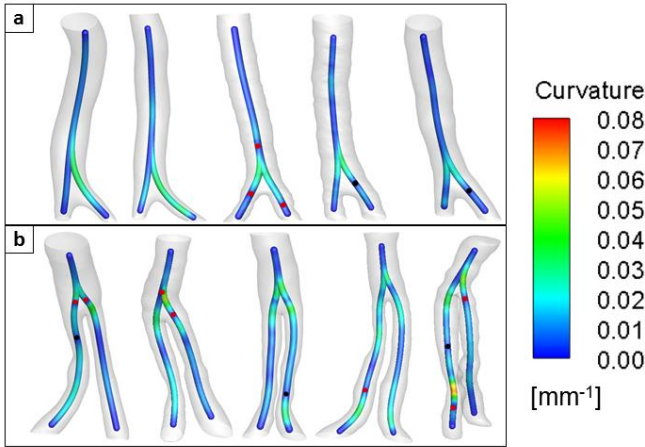


Figure 1: Centerlines with local curvature values: (a) physiological models; (b) post-operative models. Torsion peaks location are also presented (red dots, positive peaks; black dots, negative peaks).

Concerning torsion values, an inversion in sign was observed in post-operative abdominal segments (Fig. 2c). In the abdominal segment, the group averaged rate of cross-sectional area variation in post-operative models was higher than in pre-operative and healthy geometries, while an opposite trend was found in the iliac territory (Fig. 2d).

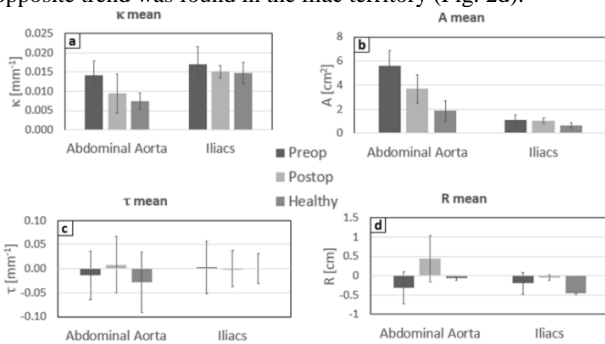


Figure 2: Group averaged values of (a) curvature, (b) cross-sectional area, (c) torsion, (d) cross-sectional area variation-rate.

As for hemodynamics, the observed group-averaged maximum WSS values (Fig. 3a) in the post-operative models were lower than the healthy cases, in the abdominal segments. In the iliac territories, a significant decrease in postoperative maximum WSS, compared to the healthy cases, was observed (8.7 ± 0.5 Pa vs 16.8 ± 1.4 Pa, $p=0.01$). The WSS contour maps (Fig. 4) confirm this finding. In post-operative cases, cycle-averaged helicity intensity in the abdominal segment of the graft was found to be higher than healthy subjects, but the difference was not statistically significant (Fig. 3b). In the iliac territories of the graft, the intensity of helical flow was close to the

healthy subjects (Fig. 3b).

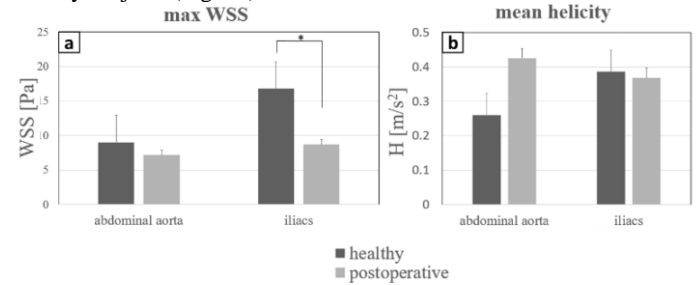


Figure 3: Group averaged (healthy and post-operative) values of (a) maximum WSS, (b) helicity intensity. (*: $p < 0.05$).

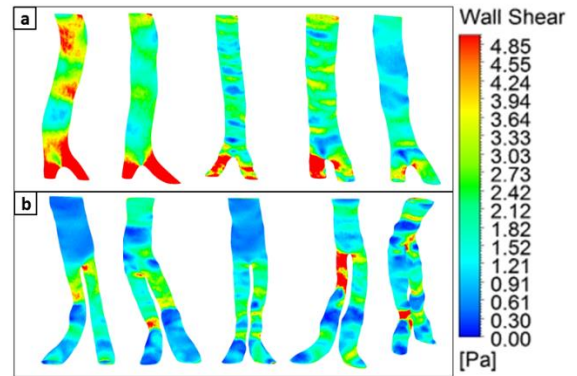


Figure 4: WSS contours at peak systole: (a) healthy cases; (b) post-operative cases (5 of the 10 investigated subjects).

DISCUSSION

The purpose of this study was: (1) to investigate the EVAR post-operative geometric reshaping; (2) to test through numerical simulations whether the geometries of endovascular repaired aortas induce significantly altered hemodynamic flow compared to healthy aortas; (3) to evaluate how vascular reshaping could influence post-operative hemodynamics. The analysis highlighted that the post-operative geometric reshaping, even if has given significant results with respect to the preoperative stage, was still far from restoring the physiological morphometry in the diseased vascular district. This was particularly true in the abdominal aorta territory, where the post-operative higher curvature, torsion sign inversion, cross-sectional area, and area variation-rate could be responsible for the enforcement of helical flow patterns in this territory, thus augmented by factors related to geometry. On the other hand, in iliac territories, where less marked morphometry differences between post-operative and healthy geometries was observed (except for the area variation-rate), comparable values of helicity intensity were observed.

The diminished maximum WSS values observed in post-operative models, with respect to healthy subjects, as well as the overall impact that EVAR has on near wall hemodynamics, and on the long term outcome of the endovascular repair is still subject of investigation, in parallel to the study of the geometric and hemodynamic impact of other commercial stent graft devices.

REFERENCES

- [1] Raptis, A et al., *Comput. Methods Biomech. Biomed. Engin.*, 0:1-8, 2016.
- [2] Gallo, D et al., *Comput. Fluid*, 141:54-61, 2016.
- [3] Olufsen, M S et al., et al., *Ann. Biomed. eng.*, 28:1281-1299, 2000.